HHS Public Access

Author manuscript

J Pers Nanomed. Author manuscript; available in PMC 2018 February 26.

Published in final edited form as:

J Pers Nanomed. 2015 November ; 1(2): 40–48.

Macrophage Targeted Nanoparticles for Antiretroviral (ARV) Delivery

Hilliard L. Kutscher[1,2,#], **Faithful Makita-Chingombe**[2,3,#], **Sara DiTursi**[2], **Ajay Singh**[1], **Admire Dube**[4], **Charles C. Maponga**[2,3], **Gene D. Morse**[2], and **Jessica L. Reynolds**[5,*]

[1]The Institute for Lasers, Photonics and Biophotonics, University at Buffalo, Buffalo, NY, USA

[2]Translational Pharmacology Research Core, New York State Center of Excellence in Bioinformatics and Life Sciences; School of Pharmacy and Pharmaceutical Sciences; University at Buffalo, Buffalo, NY, USA

[3]School of Pharmacy, University of Zimbabwe, Harare, Zimbabwe

[4]Department of Pharmaceutics, University of the Western Cape, South Africa

[5]Department of Medicine, School of Medicine and Biomedical Sciences, University at Buffalo, Buffalo NY, USA

Abstract

Objective—To reduce the amount of the antiretroviral (ARV) nevirapine necessary to achieve therapeutic concentrations using macrophage targeted nanoparticles.

Methods—Core-shell nanoparticles were prepared from FDA approved, biodegradable and biocompatible polymers, with poly(lactic-co-glycolic) acid (PLGA) as the core and chitosan (CS) as the shell using a water/oil/water method. Nevirapine was encapsulated in the core of the nanoparticles. β-glucan (GLU) was adsorbed to the surface of the nanoparticle. Macrophage uptake and intracellular nevirapine concentrations were determined by fluorescence imaging and ultra-performance liquid chromatography/mass spectroscopy (UPLC-MS). Optical imaging was employed to characterize the biodistribution of nanoparticles following intravenous injection in CD-1 mice.

Results—We synthesized spherical shaped 190 nm GLU-CS-PLGA nanoparticles that provide controlled release of nevirapine. In THP-1 macrophage the uptake of PLGA and CS- PLGA nanoparticles was less compared to targeted GLU-CS-PLGA nanoparticles. THP-1 macrophage were dosed with free nevirapine (10 μg/well) and GLU-CS- PLGA nanoparticles containing 1/10 the concentration of free nevirapine (1 μg nevirapine/well). The intracellular concentration of nevirapine was the same for both nanoparticles and free nevirapine at 2 and 24 hrs. No significant change in THP-1 macrophage viability was observed in the presence of nanoparticles relative to the control. *Ex vivo* imaging demonstrates that nanoparticles are predominantly found in the liver and kidney and at 24 hr there is still a large amount of nanoparticles in the body.

[*]Corresponding author: jlr8@bualo.edu (J.L.R.).
[#]Equal contributions

Conflicts of Interest

All authors have no conflicts of interest.

Conclusion—These data demonstrate that the total dose of nevirapine delivered by GLU-CS-PLGA nanoparticles can be greatly reduced, to limit side effects, while still providing maximal ARV activity in a known cellular reservoir.

Keywords

Nanoparticles; Nanomedicine; Macrophage; HIV; Nevirapine

Introduction

Infectious diseases are responsible for considerable morbidity and mortality, with developing countries bearing the brunt of these diseases [1]. Human immunodeficiency virus/acquired immunodeficiency syndrome (HIV/AIDS) [1], *Mycobacterium tuberculosis* (TB) [2–4] and malaria [5] rank among the most deadly of infectious diseases. The World Health Organization reported over 1.6 million deaths from HIV-1 in 2012, 1.3 million deaths from TB in 2012 and 627,000 deaths from malaria in 2012 [1–5]. In the absence of vaccines against these diseases, drug therapy approaches remain the only effective treatment option. Currently there are greater than 30 antiretrovirals (ARVs) that have been approved for the use in combination antiretroviral therapy (cART) for treatment of HIV-1 [6]. The current foundation of HIV-1 therapy is based on the combination of multiple ARVs in a single regimen. The typical first-line cART consists of two nucleoside reverse-transcriptase inhibitors (NRTI) plus a non-nucleoside reverse-transcriptase inhibitor (NNRTI) with modifications in treatment regimens if virologic failure occurs [6]. Combination therapy with highly active antiretroviral therapy (HAART) has significantly improved AIDS-related morbidity and mortality, extending the expected lifespan of patients with HIV-1 by as much as 8 to 12 years [1]. However, several factors contribute to the continuing development of treatment failure and ARV resistance, among them are: suboptimal drug efficacy and/or variable pharmacokinetics; inadequate adherence to lifelong therapy; pre-existing viral resistance to an ARV; and acute or chronic ARV toxicity [1–7].

Development of new therapies that target reservoirs of HIV-1 could potentially reduce the drug dosage required, shorten the duration of treatment, mitigate dose-dependent toxicity, and reduce the emergence of drug resistance. Macrophage are HIV-1 reservoirs which are responsible for carrying and spreading HIV-1 [8–11]. Failure to eliminate HIV-1 at cellular and tissue reservoir sites underpins the limitations of current ARV therapies. Thus the challenge of eradicating viral reservoirs, i.e., HIV-1 infected macrophage, has emerged as a fundamental barrier to the ultimate eradication of HIV-1 [11].

We designed 1,3-β-glucan (GLU) functionalized chitosan (CS) shell, poly(lactic-co-glycolic) acid (PLGA) core nanoparticles loaded with the ARV nevirapine, with a macrophage targeting ligand, GLU, on the nanoparticle surface. GLU interacts with Dectin-1, a pattern recognition receptor, on the surface of macrophages enhancing phagocytosis [12–15]. This enhanced phagocytosis has the potential to increase nanoparticle uptake and increase intracellular ARV delivery. We evaluated macrophage targeting and intracellular concentrations of nevirapine in THP-1 macrophage. We demonstrate that these functionalized nanoparticles target macrophages and that we can give nanoparticles that

contain 1/10 the concentration of free nevirapine (Free drug: 10 μg/well; GLU-CS-PLGA: 1 μg nevirapine/well) and achieve similar intracellular concentrations. These data demonstrate that the total dose of nevirapine delivered by GLU-CS-PLGA nanoparticles can be greatly reduced to limit side effects, while still providing maximal ARV activity in a known cellular reservoir of HIV-1.

Methods

Functionalized nanoparticle synthesis and characterization

Nanoparticles were fabricated using a water-oil-water (w/o/w) emulsion with solvent evaporation [16,17]. PLGA (10 mg/mL, Sigma-Aldrich, St. Louis, MO) and nevirapine (2 mg/mL, TCI America, Portland, OR) were dissolved in methylene chloride (Sigma-Aldrich) and added to 200 μL of distilled water. For cell imaging studies, Nile Red (2 mg/mL in acetone, 10 μL, Sigma-Aldrich) was added to the oil phase. For in vivo imaging studies, Cy5 (0.5 mg/mL in methylene chloride, 10 μL, Sigma-Aldrich) was added to the oil phase. The mixture was probe sonicated in a 4°C bath for 1 min followed by the rapid addition of 2 mL of 0.5% polyvinyl alcohol (Sigma-Aldrich) and probe sonicated again for 1 min. Methylene chloride was evaporated from the w/o/w emulsion under reduced pressure. The resulting suspension of PLGA nanoparticles were centrifuged at 14,000 × g for 5 minutes, decanted, and reconstituted in 2 mL of distilled water. CS (200 μL of 3 mg/mL, CS, Sigma-Aldrich) was added to the PLGA nanoparticles and the resulting CS-PLGA nanoparticles were centrifuged at 14,000 × g for 5 minutes, decanted, and reconstituted in 2 mL of distilled water. GLU (250 μL of 0.5 μg/mL GLU, Sigma-Aldrich) was added to the CS-PLGA nanoparticles and the resulting GLU-CS-PLGA nanoparticles were centrifuged at 14,000 × g for 5 minutes, decanted, and reconstituted in 2 mL of media. The size, shape, and zeta potential of the nanoparticles were characterized using dynamic light scattering (DLS) and transmission electron microscopy (TEM). The concentration of drug present in the nanoparticles was determined following extraction using acetonitrile and analyzed by UPLC-MS. Concentrations of PLGA, CS and GLU were optimized based on previous studies [16,18–21]. The amount of nevirapine used was based on the EC50 used in previous studies [22–25].

Nanoparticle characterization—The size and shape of nanoparticles was characterized using DLS and TEM. Nanoparticle size and zeta potential were determined using a Brookhaven 90 Plus Particle Analyzer (Brookhaven Instruments, Holtsville, NY) with measurements conducted at an angle of 90°. TEM images were obtained using JEOL model JEM-100CX microscope operating with acceleration voltage 80 kV. Specimens were prepared by drop-coating the nanoparticle suspension (0.1% v/v in de-ionized water) onto a holey carbon- coated 200 mesh copper grid (Electron Microscopy Sciences, Hatfield, PA) placed on filter paper to absorb excess solvent. Nanoparticles sizes were determined by Image J (1.49 software version of Image J (NIH, Bethesda, MD)) analysis of TEM images.

Drug release studies—Nevirapine release from GLU-CS-PLGA nanoparticles was performed *in vitro* in pH 7.4 phosphate buffer saline (PBS) [16]. Drug release over time was quantified using HPLC/UV. The HPLC/UV system comprised of a Waters 2795HT

Separations module (Milford, MA), connected to Waters 2996 photodiode array detector. Chromatographic separation occurred on an Atlantis dC18 (3.9 × 150 mm, 5 μm, Waters Corporation) with an Atlantis dC18 (3.9 × 20 mm, 5 um, Waters Corporation) guard column and detected using a photodiode array detector collecting at 282 nm. Chromatographic separation was performed with gradient elution. The two mobile phase components were as follows, mobile Phase A: 10 mM ammonium acetate; and mobile Phase B: 200 mL mobile phase A mixed with 500 mL of acetonitrile and 300 mL of methanol. Both mobile phases were filtered through a 0.22 μm membrane filter (EMD Millipore Corporation, Billerica, MA). The flow gradient was initially 96:4 v/v of A:B, linearly ramped to 90:10 over 8 min, 70:30 over 1.5 min; 57:43 over 3.5 min, back to 96:4 over 3.5 min and held for 6.5 min. The mobile phase flow rate was 1 mL/min, column temperature set to 40°C and injection volume was 100 μL. Data were collected and processed using Waters Empower Chromatography Software. All release studies were performed in triplicate. The calibration curve was linear over the range of 200 ng/mL to 10 μg/mL ($r^2 \geq 0.99$).

***In vitro* macrophage studies—**THP-1 macrophage were differentiated from THP-1 monocytes in the presences of phorbol 12-myristate-13-acetate (100 nM, 4 days, Sigma-Aldrich) [26].

Immunofluorescence immunostaining for Dectin-1—THP-1 macrophage (2×10^5 cells/ml) were cultured on Lab-Tek chambered cover glasses (Nalgene Nunc International, Rochester, NY), treated with nanoparticles and then were fixed and permeabilized in cold 70% methanol for 30 min at 4°C. Cells were washed in PBS, incubated with Image-iTTM FX signal enhancer (ThermoFisher Scientific) for 30 min at room temperature in a humid environment. Cells were washed in PBS then incubated with primary antibody (polyclonal goat anti-Dectin-1, Santa Cruz Biotechnology, Dallas, TX) overnight at 4°C. Cells were washed with PBS and incubated for 1 hr at room temperature with a secondary antibody conjugated to ALEXA Fluor 647 (Alexa Fluor® 647 donkey anti-goat IgG, ThermoFisher Scientific). Cells were then counterstained with the nuclear stain 4′, 6-diamidino-2-phenylindole dilactate (DAPI, ThermoFisher Scientific) and imaged by confocal microscopy using a Leica Confocal Laser Scanning Microscope (TCS SP2 AOBS, Leica Microsystems, Heidelberg GmbH) with an oil immersion objective lens 63X. An Argon 488 nm laser was applied to excite FITC; Laser operating at 405 nm was applied to excite DAPI [16].

Western blot for Dectin-1—Briefly, 50 μg of protein was separated by electrophoresis using 4–20% Tris–Hepes NuSep Longlife gels (Bioexpress, Kaysville, UT) and transferred to polyvinylidene fluoride (PVDF) membranes (Sigma-Aldrich). Membranes were blocked for 1 hr with NAP-Blocker (G-Biosciences, Maryland Heights, MO) in Tris-buffered saline with Tween 20 (150 mM NaCl, 20 mM Tris, pH 7.5, 0.1% Tween 20, TBST) and then incubated with anti-Dectin-1 primary (goat polyclonal IgG, Santa Cruz Biotechnology) overnight at 4°C with gentle rocking. After incubation with primary antibodies, membranes were washed and incubated with a biotin-conjugated secondary antibody (donkey antigoat IgG, R&D Systems, Minneapolis, MN). Membranes were washed 3 times, for 10 min each, in TBST and then incubated for 30 min with a streptavidin-alkaline phosphatase conjugate

(Invitrogen) followed by colorimetric detection using NBT/ BCIP reagent (Sigma-Aldrich) [27].

Cellular uptake of nanoparticles—Uptake of nanoparticles within THP-1 macrophage was visualized using EVOS® FL Cell Imaging System, Invitrogen. THP-1 macrophage (5×10^5 cells/ml) were cultured on 6 well tissue culture plates and incubated with Nile Red loaded PLGA, CS-PLGA, and GLU-CS-PLGA nanoparticles (100 μL of 0.1% v/v nanoparticle suspension in water based on previous studies [16,27]) for 24 hr at 37°C. Cells were then fixed with 4% paraformaldehyde at 37°C for 10 min. Cells were subsequently incubated with the nuclear stain 4′,6-diamidino-2-phenylindole (DAPI). THP-1 macrophage were imaged using EVOS® FL Cell Imaging System (ThermoFisher Scientific) at 40× magnification. The light cube used to visualize DAPI staining had an excitation of 357/44 nm and emission of 447/60 nm. The light cube use to visualize Nile Red had an excitation of 531/40 nm and emission of 593/29 nm. Quantification of imaging was performed by densitometry using Image-J.

Intracellular drug concentrations—THP-1 macrophage with incubated with free nevirapine (10 μg/ml/well) and GLU-CS-PLGA nanoparticles containing 1/10 the concentration of free nevirapine (1 μg nevirapine/well). Cells were incubated for 2 and 24 hr, cells were lysed and intracellular nevirapine was determined using a validated UPLC-MS assay. To 100 μL of cell lysate, 900 μL of acetonitrile (Sigma-Aldrich) containing internal standard (nevirapine-d3, Toronto Research Chemicals, Toronto, ON, Canada) (0.1 μg/ml), was added and centrifuged at 12 000 × g for 5 min to remove precipitated proteins and debris. Supernatant (900 μL) was dried and reconstituted in 90 μL of mobile phase A and centrifuged at 12 000 × g for 5 min to remove additional precipitated proteins and debris. Supernatant (10 μL) was injected onto a Waters Acquity UPLC-MS system for quantification. Chromatographic separation occurred on an Acquity BEH C8 (2.1 × 100 mm, 1.7 μm, Waters Corporation) and detected at m/z 267/226 with internal standard (nevirapine-d3) detected at m/z 270/229. Chromatographic separation was performed with gradient elution. The two mobile phase components were as follows, mobile Phase A: 10 mM ammonium formate adjusted to pH 4.1 with formic acid; and mobile Phase B: 0.1% formic acid in acetonitrile. Both mobile phases were filtered through a 0.22 μm membrane filter (Millipore, Milford, MA). The mobile phase flow rate was 0.4 mL/min. The flow gradient was initially 80:20 v/v of A:B for 0.40 min, linearly ramped to 20:80 over 1.2 min, held at 20:80 for 4.8 min, and then returned to 80:20 over 0.6 min. This condition was held for 3 min prior to the injection of another sample. The volume of injection was 10 μL through a 20 μL loop. Data were collected and processed using Waters MassLynx Chromatography Software. All cell uptake studies were performed in triplicate.

Cellular toxicity of nanoparticles—THP-1 macrophage (10,000 cells/ml/well) were incubated for 2 hr or 24 hr with PLGA, CS-PLGA and GLU-CS-PLGA nanoparticles. THP1 macrophage were subsequently incubated with the (3-(4,5-dimethylthiazol-2-yl)-2,5-diphenyltetrazolium bromide, (MTT) reagent for 3 hr (ThermoFisher Scientific), followed by addition of a SDS to lyse the cells and solubilize the colored crystals. Cell suspensions

were read using an ELISA plate reader (FLX800, BioTek Instruments Inc., Winooski, VT) at a wavelength of 570 nm quantifying formazan as an indicator of the number of viable cells.

Biodistribution—All mice studies were performed in AAALAC accredited animal facilities under approved protocols from the University at Buffalo Animal Use and Care Committee. Mice were fed a standard rat diet, had free access to water and were housed in a room with a 12-hr light– dark cycle for at least 1 week before the study. Nanoparticles (PLGA, CS-PLGA, GLU-CS-PLGA) were injected (100 μL, 250 μg) at time zero into CD-1 mice (20 g, female, n=3); 24 hr post-injection, mice were euthanized and organs were harvested (liver, lung, spleen, kidney) and imaged using Maestro GNIR FLEX optical imaging system (CRI, Inc., Woburn, MA). This optical system consists of an optical head that includes a liquid crystal tunable filter (LCTF, with a bandwidth of 20 nm and a scanning wavelength range of 500–950 nm) with a custom-designed, spectrally optimized lens system that relays the image to a scientific-grade megapixel CCD camera as spectral stacks. Maestro software can rapidly detect and analyze small differences in spectra between images.

Statistical analysis

Data were analyzed by the Students' *t* test using the Statistical Package for Social Science v 19 (IBM, SPSS, Chicago). Statistical differences were considered at $P < 0.05$. All data are presented as mean ± standard error of the mean (S.E.M.) unless otherwise noted.

Results

We synthesized nanoparticles with a PLGA core (PLGA) containing nevirapine surrounded by a shell of CS (CS-PLGA) with a surface macrophage targeting ligand 1,3-β-glucan (GLU-CS-PLGA). GLU targets Dectin-1, a pattern-recognition receptor on the surface of macrophage. As shown in Figure 1, dynamic light scattering (DLS) reveals the GLU-CS-PLGA nanoparticles have an approximate hydrodynamic diameter (size) of 190 nm. There was no significant difference in hydrodynamic diameter of GLU-CS-PLGA nanoparticles compared to the PLGA and CS-PLGA nanoparticles (data not shown). The zeta potential for each nanoparticle was −30 mv (PLGA), + 24 mv (CS-PLGA) and +12.47 mv (GLU-CS-PLGA). Transmission electron micrograph (TEM) (Figure 2) demonstrates the GLU-CS-PLGA nanoparticles are spherical in shape and the average size of dried nanoparticles was 96 nm. Figure 3 demonstrates that GLU-CS-PLGA nanoparticles provide controlled release of nevirapine in a pH 7.4,10 mM phosphate buffer with 95% drug released after 24 hr.

We next investigated the expression of Dectin-1, the receptor we were targeting on THP-1 macrophage. Figure 4A demonstrates the expression of Dectin-1 on THP-1 macrophage through western blotting. Figure 4B shows the immunofluorescence immunostaining for Dectin-1. Shown are representative images (a) Staining for Dectin-1 (red color) (b) corresponding bright field image. These demonstrate that Dectin-1 is expressed on THP-1 macrophage.

We next investigated intracellular uptake of PLGA, CS-PLGA, and GLU-CS-PLGA nanoparticles in THP-1 macrophage. THP-1 macrophage were incubated for 24 hr with each

nanoparticle followed by fluorescence imaging. THP-1 macrophage internalized both nontargeted (PLGA, CS-PLGA) and targeted nanoparticles (GLU-CS-PLGA) (Figure 5A). The red fluorescence arises from the encapsulation of Nile Red within the nanoparticles for imaging, and the blue fluorescence arises from DAPI staining of nuclei. Control cells are shown in a); the uptake of the b) PLGA and c) CS-PLGA nanoparticles was lower compared to the targeted d) GLU-CS-PLGA nanoparticles as seen with enhanced red color. Data shown in Figure 5B is the quantification of fluorescence performed by densitometry using Image-J. Data demonstrate that the relative fluorescent units for GLU-CS-PLGA is significantly increased compared to PLGA alone or CS-PLGA alone. Data from Figure 5 indicated that GLU is an appropriate targeting ligand that increases nanoparticle uptake in THP-1 macrophage most likely through enhanced phagocytosis.

THP-1 macrophage were then dosed with free nevirapine (10 μg/well) or GLU-CS-PLGA nanoparticles containing 1/10 the concentration of free nevirapine (1 μg nevirapine/well). Cells were incubated for 2 and 24 hr, intracellular nevirapine was determined using a validated UPLC-MS assay (Figure 6). Interestingly at both 2 hr and 24 hr, the intracellular concentration of nevirapine was the same for both nanoparticles and free nevirapine. These data suggest that the total dose of nevirapine delivered by GLU-CS-PLGA nanoparticles can be greatly reduced.

We next analyzed the cellular toxicity of the nanoparticles using an MTT assay (Figure 7). PLGA, CS-PLGA, and GLU-CS-PLGA nanoparticles were incubated with THP-1 macrophage for 2 and 24 hr, and cellular viability was determined using an MTT assay. No significant change in viability was observed in the presence of PLGA, CS-PLGA, and GLU-CS-PLGA nanoparticles relative to the control. Therefore these nanoparticles are non-toxic to THP-1 macrophage.

We next investigated the biodistribution of the nanoparticles in mice through intravenous (i.v.) tail vein injection. Nanoparticles (PLGA, CS-PLGA, GLU-CS-PLGA) were injected (100 μL, 250 μg) at time zero into CD-1 (20 g, female) mice; 24 hr post- injection, mice were euthanized and organs were harvested (liver, lung, spleen, kidney) and imaged using Maestro imaging system. Results (Figure 8) demonstrate that nanoparticles are predominantly found in the liver and kidney and at 24 hr there is still a large amount of nanoparticles in the body.

Discussion

HIV/AIDS is no longer a death sentence, but there is uncertainty concerning access and sustainability of long-term treatment, especially in resource-limited settings. Only half of the 14 million people eligible for HAART are currently receiving it [28]. A study by the CDC found that only 30% of Americans with HIV-1 are managing it properly [29]. That means 840,000 Americans have uncontrolled HIV-1 in their bodies [30]. While HIV-1 therapies has significantly improved AIDS-related morbidity and mortality, extending the expected lifespan of patients with HIV-1 [1,6] there are still limitations to these current therapies. These limitations include: (1) inability to fully eradicate HIV-1 from the body due to inadequate drug penetration into viral reservoirs; (2) a lifelong, daily regimen of medications

leading to pill fatigue and suboptimal adherence; (3) significant toxic side effects; and (4) treatment failure and ARV resistance. ARVs failure to eliminate HIV-1 at reservoir sites underpins its limitations. Thus the challenge of eradicating viral reservoirs has emerged as a fundamental barrier to the ultimate eradication of HIV-1. Latent reservoirs of HIV-1 are located throughout the body including: brain, lymphoid tissue, bone marrow, and the genital tract. The major cellular HIV-1 reservoirs are macrophage and CD4+ T cells which are responsible for carrying and spreading HIV-1 [31,32].

It is well known that a major target and reservoir of HIV-1 is CD4+ T cells, however macrophage are also HIV-1 reservoirs which are responsible for carrying and spreading HIV-1 [8,33–35]. We have chosen to target macrophage for the following reasons: (1) the lifespan of memory and effector T cells is only about 48 days while resident macrophage survive for periods of years making them ideal targets for latent HIV and also ideal cellular drug depots [36,37] and, (2) macrophage have the ability to migrate to disease sites and tissue reservoirs including the brain, making them ideal candidates for drug delivery vehicles [38,39]. Monocytes/macrophages account for around 20% of the myeloid cell type. Dectin-1, while expressed on all myeloid cell types, is highly expressed on macrophages [40,41]. Previous studies have shown that surface expression of Dectin-1 is increased when macrophage are activated [42]. Macrophage activation is known to be modulated by HIV-1 [8,9,38,43], therefore the expression of Dectin-1 on macrophage is likely to be modulated in HIV-1. With such knowledge we designed a functionalized nanoparticle with surface bound GLU that targets Dectin-1 on the surface of macrophage. We synthesized spherical shaped 190 nm mean sized nanoparticles, composed of CS-PLGA that were functionalized with GLU. This nanoparticle provided controlled release of nevirapine in PBS with pH mimicking plasma and cytoplasmic pH of cells. In THP-1 macrophages, we observed that the presence of GLU enhanced the uptake of the nanoparticles by macrophage. Therefore, GLU functionalized PLGA nanoparticles are more advantageous for macrophage targeted drug delivery than non-targeted PLGA nanoparticles. In our previous study, we observed a similar enhancement in nanoparticle uptake by human derived alveolar like macrophages following GLU functionalization [16]. It is known that GLU preferentially binds to the lectin type receptor Dectin-1 expressed in high concentrations on macrophage surfaces [44]. This binding increases nanoparticle uptake most likely through enhanced phagocytosis [16]. The interaction of curdlan (a linear chain GLU) functionalized PLGA nanoparticles with THP-1 derived macrophages has been characterized through real-time cell impedance measurements and has been shown to result in Ca2+ dependent phagocytosis by the macrophages [45]. Hence the results of this study support these prior works and it is likely that the enhanced nanoparticle uptake observed is due to GLU activation of Dectin-1.

We previously demonstrated using a similar nanoparticle that intracellular concentrations of rifampin, a TB drug, were increased in macrophage when delivered by nanoparticles. Free rifampin and rifampin loaded (GLU-CS-PLGA) nanoparticles were incubated with monocyte derived macrophage (MDM) to give a total rifampin mass of 5 μg/well. Nanoparticles increased intracellular rifampin concentration by 4-fold in macrophage compared to rifampin solution [16]. In this study, we investigated the dose of nanoparticles necessary to deliver intracellular nevirapine similar to free drugs. It was interesting to note that the nanoparticles could achieve intracellular concentrations of nevirapine which were

similar to free nevirapine over a 24 hr period, at only 1/10th of the dose. We attribute this observation to the enhanced uptake of the drug loaded nanoparticles by the macrophages. This finding suggests that the total dose of nevirapine can be greatly reduced through delivery by GLU-CS-PLGA nanoparticles to limit side effects, while still providing maximal ARV activity in a known cellular reservoir. To confirm this, in future studies using animal models, we will assess bioavailability and pharmacokinetics of the drug loaded nanoparticles to assess the tissue and cellular nevirapine concentrations delivered by the nanoparticles.

Animal biodistribution studies are an important part of the characterization of the drug delivery capability of nanoparticle systems. Our ex vivo biodistribution studies demonstrate that our nanoparticles are predominantly found in the liver and kidney, and at 24 hr there is still a large amount of nanoparticles in the body indicating the potential of nanoparticles to increase the overall residence time of drug in the body. The liver, kidney, lung and spleen are known reticuloendothelial system sites and the data therefore, suggests opsonization of the nanoparticles and phagocytosis and clearance by monocytes and macrophages [46]. Previous studies have shown that macrophage can be intracellular depots for ARVs and these macrophage subsequently deliver ARV to HIV-1 reservoirs sites [34,39, 47–53]. It is our goal to target macrophages, which are migratory by nature and therefore, can serve as drug carriers to various organs in the body. The research group led by Howard Gendelman has demonstrated a NanoART drug delivery system, targeted towards macrophages which act as drug depots; these macrophage then distribute drugs to cellular and tissue HIV-1 reservoirs including lymph nodes, gut and the brain where they reduce viral load, providing long acting pharmacokinetic characteristics [34,39,47–53]. Our nanoparticle system has demonstrated potential to function in a similar way, with the added advantage of enhanced macrophage uptake (through Dectin-1 activation by GLU) and reduced dose requirements. Furthermore, we have previously shown that our nanoparticle system activates the innate immune system, increasing production of proinflammatory cytokines and generation of reactive oxygen and reactive nitrogen species (ROS/RNS) [16]. Studies have shown that activation of TLR receptors, production of cytokines and ROS/RNS differentially modulate latent HIV-1 [43,54]; therefore activation of these macrophage by GLU on the surface of our nanoparticle system may enhance viral clearance.

This study lays the foundation for a new treatment approach towards HIV-1 that reduces the necessary dose of ARVs used. We believe that this nanoparticle will be an excellent adjuvant when given with standard ARV treatment. Our future studies will investigate in vitro and in vivo models of HIV-1 infection and advance the pre-clinical investigation of these nanoparticles in anticipation of providing complete combination regimens for HIV-1.

Acknowledgments

Funding Support

This project was supported in part by the University of Rochester Center for AIDS Research grant P30AI078498 (NIH/ NIAID) and the University of Rochester School of Medicine and Dentistry. Additional support was received from the following grants: grant U01AI068636 and R56AI114298 (JR) from the National Institutes of Health, National Institute of Allergy and Infectious Diseases (NIAID). FM is a fellow supported by a grant D43TW007991 (GM) from the National Institutes of Health, Fogarty International Center, AIDS International Training and Research Program (AITRP). HK is supported by Ruth L. Kirschstein National Research Service Award (NRSA) Institutional Research Training Grant 1T32GM099607.

The collaborative contributions and dedication of the research staff from the Translational Pharmacology Research Core at the University at Buffalo is appreciated. We would also like to express our appreciation to Waters Corporation for their generous HPLC and ACQUITY UPLC/TQD LC-MS/MS system donation. The content presented in this paper is solely the responsibility of the authors and does not necessarily represent the official views of the Fogarty International Center, National Institute of Allergy and Infectious Diseases, or the National Institutes of Health.

References

1. HIV/AIDS, Fact sheet N°360, Updated October 2013.
2. Tuberculosis, Fact sheet, October 2013.
3. Global tuberculosis report 2013.
4. TB/HIV, 2013.
5. Malaria, Fact sheet N°94, Updated December 2013.
6. Consolidated ARV guidelines, June 2013.
7. Cohen K, Meintjes G. Management of individuals requiring antiretroviral therapy and TB treatment. Curr Opin HIV AIDS. 2010; 5:61–69. [PubMed: 20046149]
8. Abbas W, Tariq M, Iqbal M, Kumar A, Herbein G. Eradication of HIV-1 from the macrophage reservoir: an uncertain goal? Viruses. 2015; 7:1578–1598. [PubMed: 25835530]
9. Gartner S. The macrophage and HIV: basic concepts and methodologies. Methods Mol Biol. 2014; 1087:207–220. [PubMed: 24158825]
10. Kumar A, Herbein G. The macrophage: a therapeutic target in HIV-1 infection. Mol Cell Ther. 2014; 2:10. [PubMed: 26056579]
11. Swami M. HIV infections: Restricting HIV from macrophages. Nature Medicine. 2013; 19:416–416.
12. Batbayar S, Lee DH, Kim HW. Immunomodulation of Fungal beta-Glucan in Host Defense Signaling by Dectin-1. Biomol Ther (Seoul). 2012; 20:433–445. [PubMed: 24009832]
13. Goodridge HS, Underhill DM, Touret N. Mechanisms of Fc receptor and dectin-1 activation for phagocytosis. Traf c. 2012; 13:1062–1071.
14. Plato A, Willment JA, Brown GD. C-type lectin-like receptors of the dectin-1 cluster: ligands and signaling pathways. Int Rev Immunol. 2013; 32:134–156. [PubMed: 23570314]
15. Saijo S, Iwakura Y. Dectin-1 and Dectin-2 in innate immunity against fungi. Int Immunol. 2011; 23:467–472. [PubMed: 21677049]
16. Dube ARJ, Law WC, Maponga CC, Prasad PN, Morse GD. Multimodal Nanoparticles that Provide Immunomodulation and Intracellular Drug Delivery for Infectious Diseases. Nanomedicine: Nanotechnology, Biology, and Medicine. 2014
17. Prasad, PN. Introduction To Nanomedicine And Nanobioengineering. Wiley; New Jersey: 2012.
18. Nkabinde LA, Shoba-Zikhali LNN, Semete-Makokotlela B, Kalombo L, Swai HS, Hayeshi R, et al. Permeation of PLGA Nanoparticles Across Different in vitro Models. Current Drug Delivery. 2012; 9:617–627. [PubMed: 22812395]
19. Semete B, Booysen L, Kalombo L, Ramalapa B, Hayeshi R, Swai HS. Effects of protein binding on the biodistribution of PEGylated PLGA nanoparticles post oral administration. International Journal of Pharmaceutics. 2012; 424:115–120. [PubMed: 22227605]
20. Semete B, Booysen L, Lemmer Y, Kalombo L, Katata L, Verschoor J, et al. In vivo evaluation of the biodistribution and safety of PLGA nanoparticles as drug delivery systems. Nanomedicine: Nanotechnology, Biology and Medicine. 2010; 6:662–671.
21. Stigliano CAS, de Tullio MD, Nicchia GP, Pascazio G, Svelto M, Decuzzi P. siRNA chitosan complexes in poly(lactic-co-glycolic acid) nanoparticles for the silencing of aquaporin-1 in cancer cells. Mol Pharm. 2013; 10:3186–3194. [PubMed: 23789777]
22. Cheeseman SHHS, McLaughlin MM, Koup RA, Andrews C, Bova CA, Pav JW, Roy T, Sullivan JL, Keirns JJ. Pharmacokinetics of Nevirapine: Initial Single-Rising-Dose Study in Humans. Antimicrob Agents Chemother. 1993; 37:178–182. [PubMed: 8452345]

23. Grob PMWJ, Cohen KA, Ingraham RH, Shih CK, Hargrave KD, McTague TL, Merluzzi VJ. Nonnucleoside inhibitors of HIV-1 reverse transcriptase: nevirapine as a prototype drug. AIDS Res Hum Retroviruses. 1992; 8:145–152. [PubMed: 1371691]
24. Sriram DYP, Kishore MR. Synthesis and anti-HIV activity of nevirapine prodrugs. Pharmazie. 2006; 61:895–897. [PubMed: 17152978]
25. Palaniappan CFP, Bambara RA. Nevirapine alters the cleavage specificity of ribonuclease H of human immunodeficiency virus 1 reverse transcriptase. J Biol Chem. 1995; 270:4861–4869. [PubMed: 7533167]
26. Essaji Y, Yang Y, Albert CJ, Ford DA, Brown RJ. Hydrolysis products generated by lipoprotein lipase and endothelial lipase differentially impact THP-1 macrophage cell signalling pathways. Lipids. 2013; 48:769–778. [PubMed: 23794138]
27. Reynolds JL, Law WC, Mahajan SD, Aalinkeel R, Nair B, Sykes DE, et al. Morphine and galectin-1 modulate HIV-1 infection of human monocyte-derived macrophages. J Immunol. 2012; 188:3757–3765. [PubMed: 22430735]
28. Society IA. Living with HIV is no longer a death sentence so why do we need a cure?.
29. CDC. HIV in the United States: At A Glance. 2014.
30. Hall HEF, Rhodes P, Holtgrave D, Furlow-Parmley C, Tang T, Gray K, Cohen S, Mermin J, Skarbinski J. Differences in Human Immunodeficiency Virus Care and Treatment Among Subpopulations in the United States. JAMA Intern Med. 2013; 173:1337–1344. [PubMed: 23780395] JAMA Intern Med. 2013; 173:1337–1344. [PubMed: 23780395]
31. Mitsuhashi M, Taub DD, Kapogiannis D, Eitan E, Zukley L, Mattson MO, et al. Aging enhances release of exosomal cytokine mRNAs by AB1-42-stimulated macrophages. FASEB J. 2013; 27:5141–5150. [PubMed: 24014820]
32. Xing S, Siliciano RF. Targeting HIV latency: pharmacologic strategies toward eradication. Drug Discov Today. 2013; 18:541–551. [PubMed: 23270785]
33. Bruner KMHN, Siliciano RF. Towards an HIV-1 cure: measuring the latent reservoir. Trends Microbiol. 2015; 23:192–203. [PubMed: 25747663]
34. Edagwa BJZT, McMillan JM, Liu XM, Gendelman HE. Development of HIV reservoir targeted long acting nanoformulated antiretroviral therapies. Curr Med Chem. 2014; 21:4186–4198. [PubMed: 25174930]
35. Peyron P, Vaubourgeix J, Poquet Y, Levillain F, Botanch C, Bardou F, Daffé M, Emile J, Marchou B, Cardona P, de Chastellier C, Altare F. Foamy macrophages from tuberculous patients granulomas constitute a nutrient-rich reservoir for M. tuberculosis persistence. PLOS Pathogens. 2008; 4:e1000204. [PubMed: 19002241]
36. Tough DFSJ. Life span of naive and memory T cells. Stem Cells. 1995; 13:242–249. [PubMed: 7613491]
37. Parihar A, Eubank TD, Doseff AI. Monocytes and macrophages regulate immunity through dynamic networks of survival and cell death. J Innate Immun. 2010; 2:204–215. [PubMed: 20375558]
38. Schultze JL, Schmieder A, Goerdt S. Macrophage activation in human diseases. Semin Immunol. 2015
39. Araínga MGD, Wiederin J, Ciborowski P, McMillan J, Gendelman HE. Opposing regulation of endolysosomal pathways by long-acting nanoformulated antiretroviral therapy and HIV-1 in human macrophages. Retrovirology. 2015; doi: 10.1186/s1297712014-10133-12975.
40. Brown GD, Taylor PR, Reid DM, Willment JA, Williams DL, Martinez-Pomares L, et al. Dectin-1 Is A Major-Glucan Receptor On Macrophages. Journal of Experimental Medicine. 2002; 196:407–412. [PubMed: 12163569]
41. Taylor PR, Brown GD, Reid DM, Willment JA, Martinez-Pomares L, Gordon S, et al. The Glucan Receptor, Dectin-1, Is Predominantly Expressed on the Surface of Cells of the Monocyte/Macrophage and Neutrophil Lineages. The Journal of Immunology. 2002; 169:3876–3882. [PubMed: 12244185]
42. Willment JA, Lin HH, Reid DM, Taylor PR, Williams DL, Wong SYC, et al. Dectin-1 Expression and Function Are Enhanced on Alternatively Activated and GM-CSF-Treated Macrophages and

Are Negatively Regulated by IL-10, Dexamethasone, and Lipopolysaccharide. The Journal of Immunology. 2003; 171:4569–4573. [PubMed: 14568930]

43. Lane BRMD, Woodford NL, Rochford R, Strieter RM, Coffey MJ. TNF-alpha inhibits HIV1 replication in peripheral blood monocytes and alveolar macrophages by inducing the production of RANTES and decreasing C-C chemokine receptor 5 (CCR5) expression. J Immunol. 1999; 163:3653–3661. [PubMed: 10490959]
44. Brown GD, Taylor PR, Reid DM, Willment JA, Williams DL, Martinez-Pomares L, et al. Dectin-1 Is A Major β-Glucan Receptor On Macrophages. The Journal of Experimental Medicine. 2002; 196:407–412. [PubMed: 12163569]
45. Tukulula M, Hayeshi R, Fonteh P, Meyer D, Ndamase A, Madziva M, et al. Curdlan Conjugated PLGA Nanoparticles Possess Macrophage Stimulant Activity and Drug Delivery Capabilities. Pharmaceutical Research. 2015; 32:2713–2726. [PubMed: 25724161]
46. Owens DE Iii, Peppas NA. Opsonization, biodistribution, and pharmacokinetics of polymeric nanoparticles. International Journal of Pharmaceutics. 2006; 307:93–102. [PubMed: 16303268]
47. Gautam N, Roy U, Balkundi S, Puligujja P, Guo D, Smith N, et al. Preclinical pharmacokinetics and tissue distribution of long-acting nanoformulated antiretroviral therapy. Antimicrob Agents Chemother. 2013; 57:3110–3120. [PubMed: 23612193]
48. Gautam NPP, Balkundi S, Thakare R, Liu XM, Fox HS, McMillan J, Gendelman HE, Alnouti Y. Pharmacokinetics, biodistribution, and toxicity of folic acid-coated antiretroviral nanoformulations. Antimicrob Agents Chemother. 2014; 58(12):7510–7519. [PubMed: 25288084]
49. Kingsley J, Dou H, Morehead J, Rabinow B, Gendelman H, Destache C. Nanotechnology: A Focus on Nanoparticles as a Drug Delivery System. Journal of Neuroimmune Pharmacology. 2006; 1:340–350. [PubMed: 18040810]
50. Li TGH, Zhang G, Puligujja P, McMillan JM, Bronich TK, Edagwa B, Liu XM, Boska MD. Magnetic resonance imaging of folic acid-coated magnetite nanoparticles reflects tissue biodistribution of long-acting antiretroviral therapy. Int J Nanomedicine. 2015; 10:37793790.
51. Puligujja PAM, Dash P, Palandri D, Mosley RL, Gorantla S, Poluektova L, McMillan J, Gendelman HE. Pharmacodynamics of folic acid receptor targeted antiretroviral nanotherapy in HIV- 1-infected humanized mice. Antiviral Res. 2015; 120:85–88. [PubMed: 26026666]
52. Puligujja PBS, Kendrick LM, Baldridge HM, Hilaire JR, Bade AN, Dash PK, Zhang G, Poluektova LY, Gorantla S, Liu XM, Ying T, Feng Y, Wang Y, Dimitrov DS, McMillan JM, Gendelman HE. Pharmacodynamics of long-acting folic acid- receptor targeted ritonavir boosted atazanavir nanoformulations. Biomaterials. 2014; 41:141–150. [PubMed: 25522973]
53. Ross KABT, Binnebose AM, Phanse Y, Kanthasamy AG, Gendelman HE, Salem AK, Bartholomay LC, Bellaire BH, Narasimhan B. Nano-Enabled Delivery of Diverse Payloads Across Complex Biological Barriers. J Control Release. 2015:S0168–3659.
54. Novis CLAN, Buzon MJ, Verdin E, Round JL, Lichterfeld M, Margolis DM, Planelles V, Bosque A. Reactivation of latent HIV-1 in central memory CD4+ T cells through TLR-1/2 stimulation. Retrovirology. 2013:10. [PubMed: 23369348]

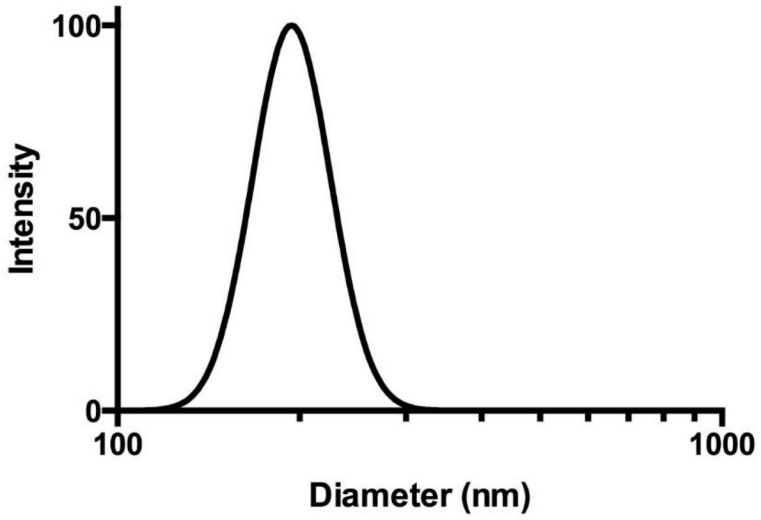

Figure 1.

Characterization of GLU-CS-PLGA nanoparticle through dynamic light scattering (DLS). The average size of the nanoparticles was 190 nm.

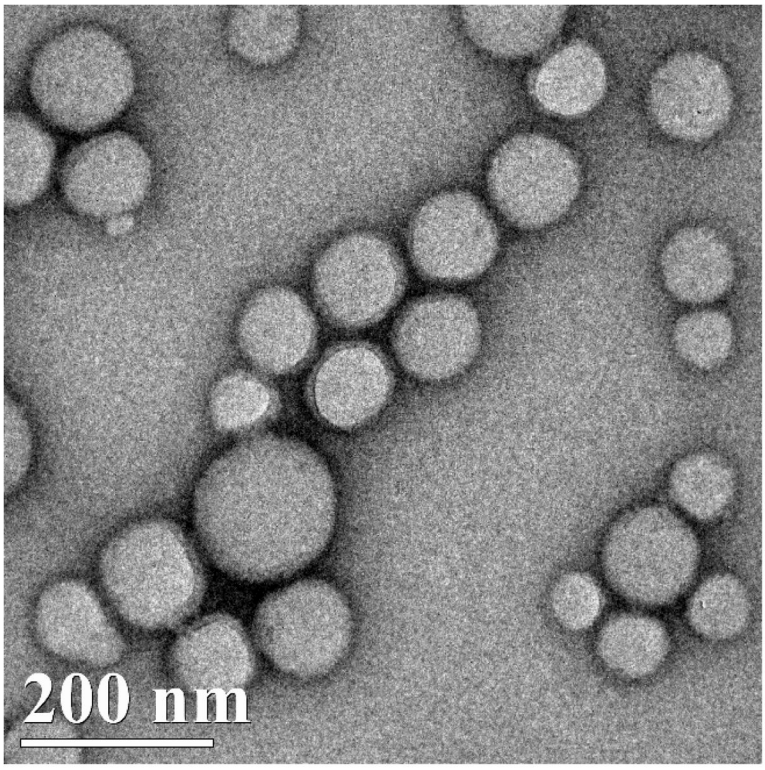

Figure 2.
TEM of nevirapine loaded GLU-CS-PLGA nanoparticles. The average diameter (size) of GLU-CS-PLGA nanoparticles observed by TEM was 96 nm.

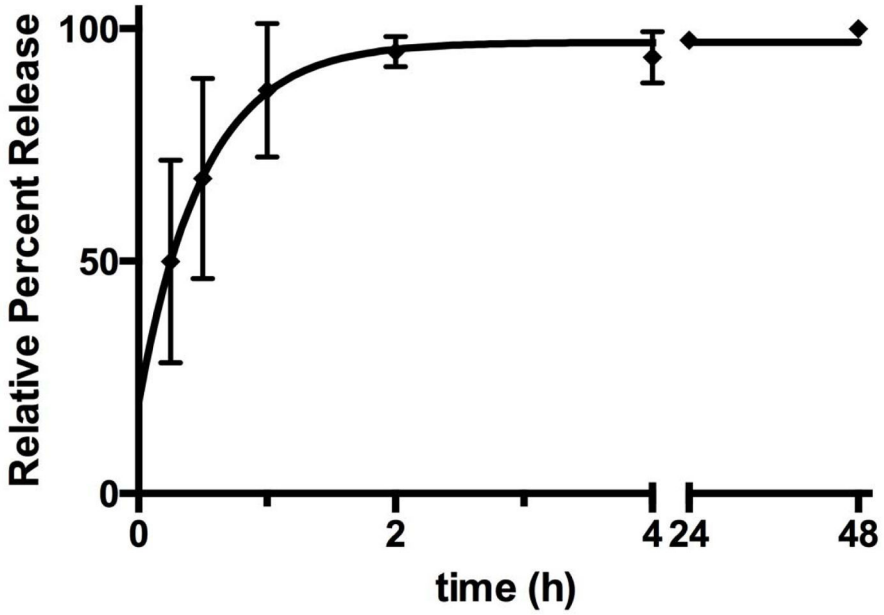

Figure 3.
Release kinetics of nevirapine over time from GLU-CS-PLGA nanoparticles.

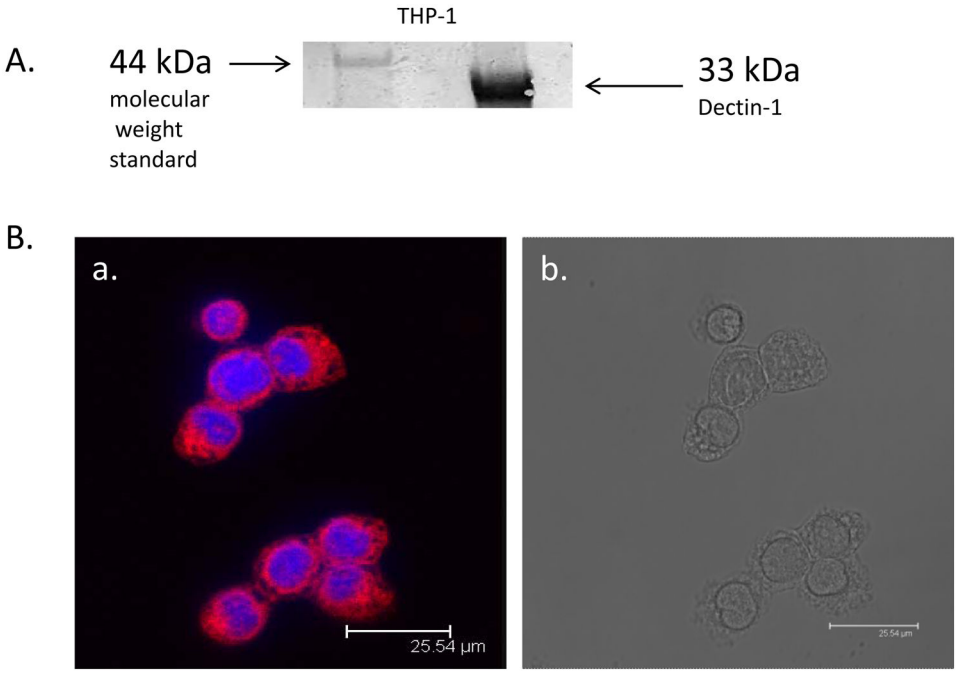

Figure 4.

Protein expression of Dectin-1 in THP-1 macrophage. A). Representative western blot for both Dectin-1 in THP-1 macrophage, Dectin-1 is approximately 33 kDa in size; B) Immunofluorescent immunostaining for Dectin-1. Representative confocal image of Dectin-1 protein expression. (a) Positive staining for Dectin-1 in THP-1 macrophage (b) corresponding bright field image.

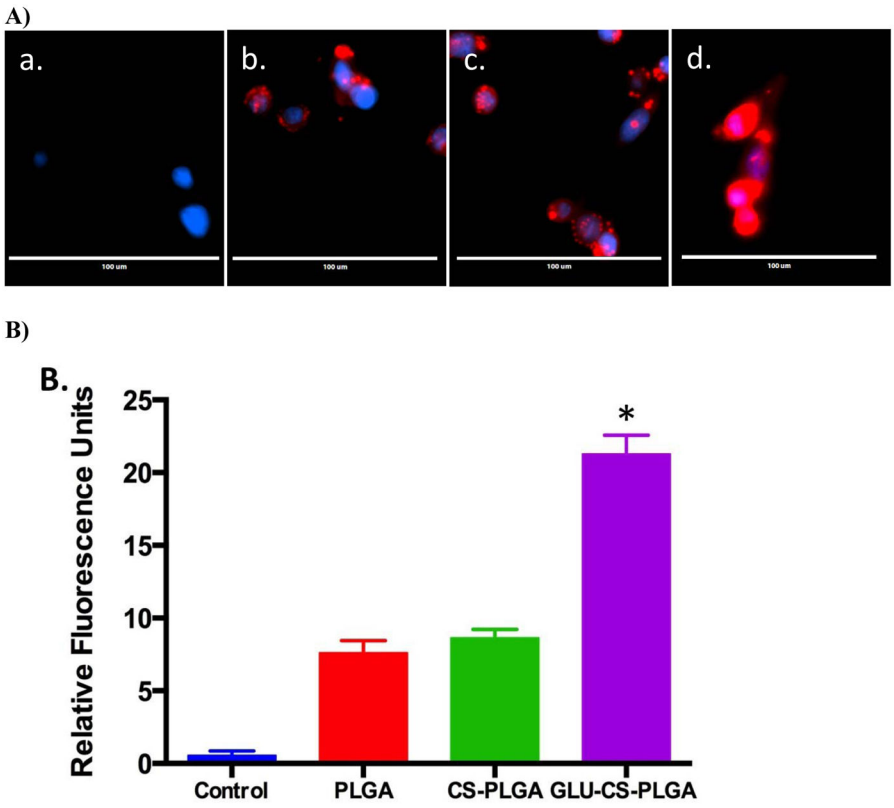

Figure 5.

Uptake of PLGA, CS-PLGA, and GLU-CS-PLGA nanoparticles in THP-1 macrophage after 24 hr incubation. A) Representative EVOS Images. The red fluorescence arises from the Nile Red loaded nanoparticles, and the blue fluorescence arises from DAPI staining of nuclei Representative 40X magnification a) control; b) PLGA; c) CS-PLGA; d) GLU-CS-PLGA. B) Quantification of fluorescent imaging was performed by densitometry using Image-J. Data are presented as relative fluorescent units.

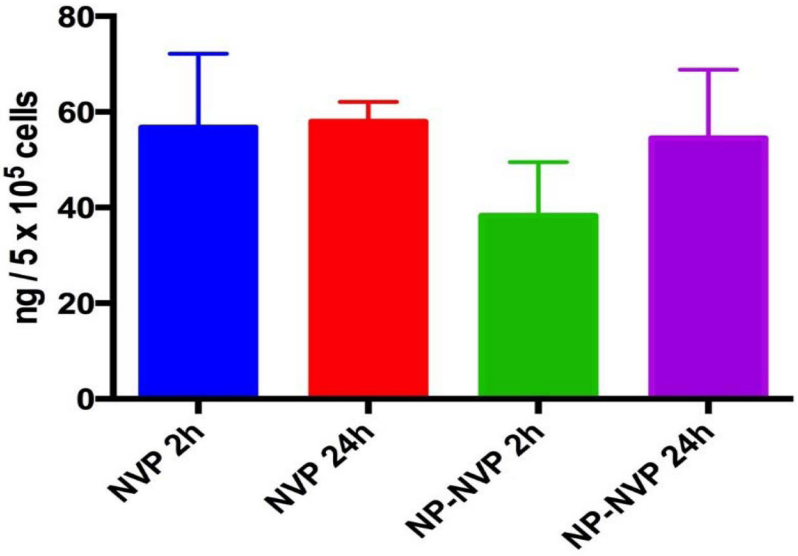

Figure 6.
Intracellular concentrations of nevirapine delivered by GLU-CS-PLGA nanoparticles. NVP = free nevirapine; NP-NVP = nanoparticle with nevirapine.

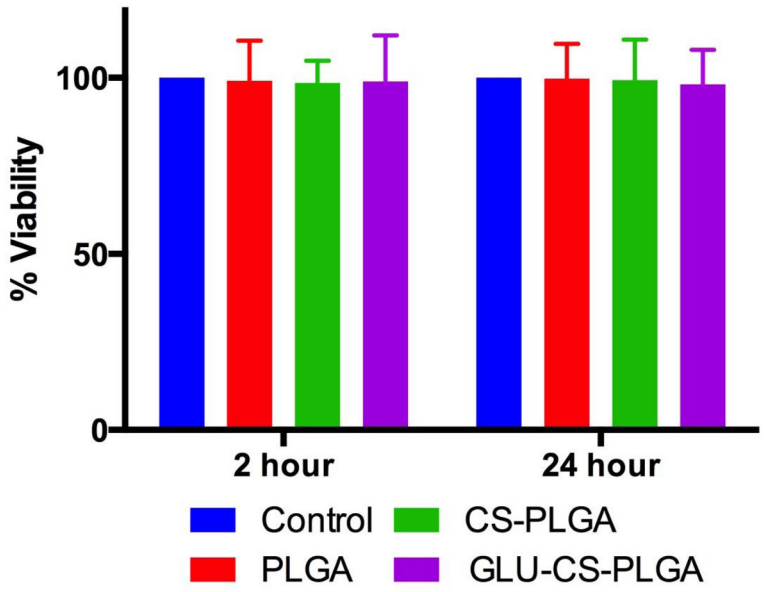

Figure 7.

Cell viability of THP-1 macrophage after exposure to PLGA, CS-PLGA, and GLU-CS-PLGA nanoparticles. THP-1 macrophage were incubated for 2 hr and 24 hr with PLGA, CS-PLGA, and GLU-CS- PLGA nanoparticles and analyzed for cell viability using an MTT assay.

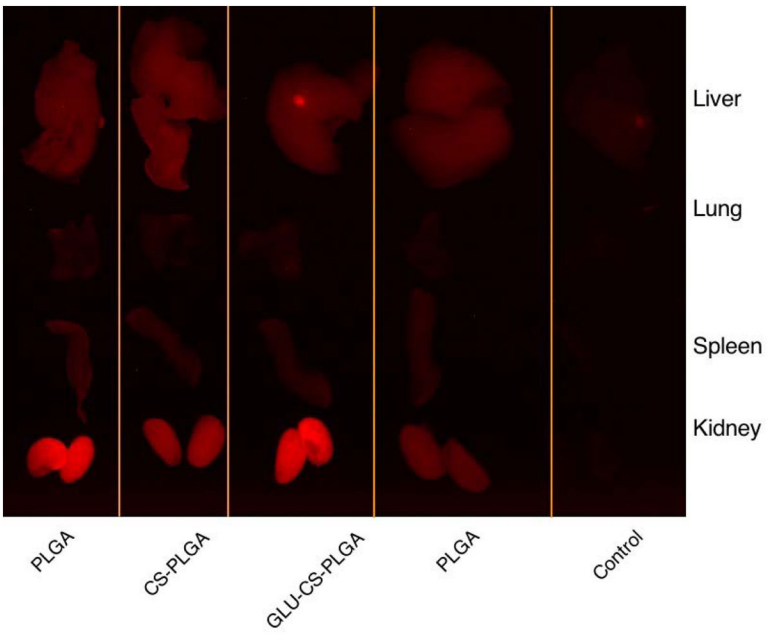

Figure 8.

Ex vivo bio-distribution following i.v. tail vein injection; (1) CS-PLGA (2) GLU-CS-PLGA (3) PLGA (4) Control.